



## Research Article

## Korean Red Ginseng aqueous extract improves markers of mucociliary clearance by stimulating chloride secretion

Do-Yeon Cho<sup>1,2,\*,\*,☆</sup>, Daniel Skinner<sup>1</sup>, Shaoyan Zhang<sup>1</sup>, Ahmed Lazrak<sup>2,3</sup>, Dong Jin Lim<sup>1</sup>, Christopher G. Weeks<sup>1</sup>, Catherine G. Banks<sup>1</sup>, Chang Kyun Han<sup>4</sup>, Si-Kwan Kim<sup>5</sup>, Guillermo J. Tearney<sup>6</sup>, Sadis Matalon<sup>2,3</sup>, Steven M. Rowe<sup>2,7</sup>, Bradford A. Woodworth<sup>1,2,\*,\*,☆</sup>

<sup>1</sup> Department of Otolaryngology Head & Neck Surgery, University of Alabama at Birmingham, Birmingham, Alabama, United States

<sup>2</sup> Gregory Fleming James Cystic Fibrosis Research Center, University of Alabama at Birmingham, Birmingham, Alabama, United States

<sup>3</sup> Department of Anesthesiology and Perioperative Medicine, University of Alabama at Birmingham, Birmingham, Alabama, United States

<sup>4</sup> Korea Ginseng Research Institute, Korea Ginseng Corporation, Daejeon, Republic of Korea

<sup>5</sup> Department of Biomedical Chemistry, Konkuk University, Chungju, Republic of Korea

<sup>6</sup> Wellman Center for Photomedicine, Massachusetts General Hospital, Boston, Massachusetts, United States

<sup>7</sup> Departments of Medicine, Pediatrics, Cell Developmental and Integrative Biology, University of Alabama at Birmingham, Birmingham, Alabama, United States

## ARTICLE INFO

## Article history:

Received 16 August 2018

Received in Revised form

30 August 2019

Accepted 6 September 2019

Available online 13 September 2019

## Keywords:

CFTR

Chloride channels

Mucociliary clearance

Red Ginseng

Sinusitis

## ABSTRACT

**Background:** Abnormal chloride ( $\text{Cl}^-$ ) transport has a detrimental impact on mucociliary clearance in both cystic fibrosis (CF) and non-CF chronic rhinosinusitis. Ginseng is a medicinal plant noted to have anti-inflammatory and antimicrobial properties. The present study aims to assess the capability of red ginseng aqueous extract (RGAE) to promote transepithelial  $\text{Cl}^-$  secretion in nasal epithelium.

**Methods:** Primary murine nasal septal epithelial (MNSE) [wild-type (WT) and transgenic CFTR<sup>-/-</sup>], fisher-rat-thyroid (FRT) cells expressing human WT CFTR, and TMEM16A-expressing human embryonic kidney cultures were utilized for the present experiments. Ciliary beat frequency (CBF) and airway surface liquid (ASL) depth measurements were performed using micro-optical coherence tomography ( $\mu\text{OCT}$ ). Mechanisms underlying transepithelial  $\text{Cl}^-$  transport were determined using pharmacologic manipulation in Ussing chambers and whole-cell patch clamp analysis.

**Results:** RGAE (at 30  $\mu\text{g}/\text{mL}$  of ginsenosides) significantly increased  $\text{Cl}^-$  transport [measured as change in short-circuit current ( $\Delta I_{\text{SC}} = \mu\text{A}/\text{cm}^2$ )] when compared with control in WT and CFTR<sup>-/-</sup> MNSE (WT vs control =  $49.8 \pm 2.6$  vs  $0.1 \pm 0.2$ , CFTR<sup>-/-</sup> =  $33.5 \pm 1.5$  vs  $0.2 \pm 0.3$ ,  $p < 0.0001$ ). In FRT cells, the CFTR-mediated  $\Delta I_{\text{SC}}$  attributed to RGAE was small ( $6.8 \pm 2.5$  vs control,  $0.03 \pm 0.01$ ,  $p < 0.05$ ). In patch clamp, TMEM16A-mediated currents were markedly improved with co-administration of RGAE and uridine 5-triphosphate ( $8406.3 \pm 807.7$  pA) over uridine 5-triphosphate ( $3524.1 \pm 292.4$  pA) or RGAE alone ( $465.2 \pm 90.7$  pA) ( $p < 0.0001$ ). ASL and CBF were significantly greater with RGAE ( $6.2 \pm 0.3$   $\mu\text{m}$  vs control,  $3.9 \pm 0.09$   $\mu\text{m}$ ;  $10.4 \pm 0.3$  Hz vs control,  $7.3 \pm 0.2$  Hz;  $p < 0.0001$ ) in MNSE.

**Conclusion:** RGAE augments ASL depth and CBF by stimulating  $\text{Cl}^-$  secretion through CaCC, which suggests therapeutic potential in both CF and non-CF chronic rhinosinusitis.

© 2019 The Korean Society of Ginseng, Published by Elsevier Korea LLC. This is an open access article under the CC BY-NC-ND license (<http://creativecommons.org/licenses/by-nc-nd/4.0/>).

## 1. Introduction

Sinonasal mucociliary transport is a vital host defense mechanism that dispels inhaled pathogens such as toxins, allergens, and

pollutants from the airway [1,2]. Airway epithelium sustains mucociliary function through proper ciliary beating and homeostatic maintenance of the airway surface liquid (ASL) [1,3]. ASL and the viscoelastic characteristics of the mucus rely on the

\* Corresponding author. Department of Otolaryngology – Head and Neck Surgery University of Alabama at Birmingham DB 563, 1720 2nd Avenue S, Birmingham, AL, 35294-0012, United States.

\*\* Corresponding author. Department of Otolaryngology Head & Neck Surgery, University of Alabama at Birmingham, Birmingham, Alabama, United States.

E-mail addresses: [dycho@uabmc.edu](mailto:dycho@uabmc.edu) (D.-Y. Cho), [bwoodwo@uab.edu](mailto:bwoodwo@uab.edu) (B.A. Woodworth).

☆ Do-Yeon Cho, MD receives research grant support from Bionorica Inc. and Bradford A. Woodworth, M.D. is a consultant for Olympus and Cook Medical. He also receives grant support from Cook Medical and Bionorica Inc.

synchronized action of multiple ion channels, including the cystic fibrosis transmembrane conductance regulator (CFTR) and calcium activated chloride channels (CaCC) [*TMEM16A* (*Anoctamin1* or ANO1) and *TMEM16B* (*Anoctamin2* or ANO2)] [4–6].

Because mucociliary transport is influenced by the trans-epithelial movement of chloride ( $\text{Cl}^-$ ), there is increasing interest in the use of agents that stimulate  $\text{Cl}^-$  secretion for the treatment of diseases caused by dysfunctional mucociliary clearance (MCC), including cystic fibrosis (CF), chronic obstructive pulmonary disease, asthma, and chronic rhinosinusitis [7–11]. While several drugs targeting CFTR have been approved by the Food and Drug Administration for CF disease (e.g., ivacaftor, lumacaftor), compounds from natural products are also being explored, ranging from extracts of South Pacific sponges to plants in local health food stores [12,13]. For example, genistein, curcumin, and resveratrol have been evaluated for their potential as adjunct therapies for patients with CF as they show the capacity to stimulate CFTR as channel potentiators [14–16]. Modulators of CaCC activity, such as uridine 5-triphosphate (UTP) and other analogues, have also been considered for the treatment of CF and additional airway diseases [17,18].

Korean Red Ginseng (*Panax ginseng* Meyer) is widely used as an alternative medicine and health-enhancing supplement [19]. Commercially available Korean Red Ginseng aqueous extract (RGAE) is prepared by steaming and drying fresh ginseng root to enrich efficacy and is composed of several unique ginsenosides (Rg1, Rb1, Rg3) derived from hydrolysis of saponins during heating procedures [20]. Ginsenosides are regarded as the principle active compounds of *P. ginseng* and have been recognized to have anti-inflammatory, antioxidant and antimicrobial bioactivity [20–22]. A recent study by Guo et al. has shown that ginsenoside Rb1 can activate CaCCs in the Guinea pig's intestine [22]. In a study with tissue distribution profiles, the two organs with the highest levels of ginsenosides were liver and lung after oral administration in a rat model [23]. However, data regarding the electrophysiologic characteristics of RGAE in the respiratory tract are lacking. The objectives of this study are to assess the capability of RGAE to promote transepithelial  $\text{Cl}^-$  secretion in sinonasal epithelium.

## 2. Materials and methods

### 2.1. Primary cell culture

Institutional Animal Care and Use Committee and Institutional Review Board approvals were obtained before initiating these studies. Murine nasal septal epithelial (MNSE) cells were matured on Costar 6.5-mm-diameter permeable filters (Corning Life Sciences, Lowell, MA, USA) and immersed in culture medium as previously described [2,24–28]. The medium was drained from the apical surface on day 4 after the epithelium reached confluence, and cells fed via the basal chamber. Transgenic CFTR<sup>-/-</sup> MNSE cultures were also studied to assess CFTR-dependent effects and appraise contributions from apical CaCC. Differentiation and ciliogenesis arose in all cultures within 10 to 14 days. Cultures were used for experiments when fully differentiated with prevalent ciliogenesis. Cultures with transepithelial resistances ( $R_t$ ) > 300  $\Omega \cdot \text{cm}^2$  were used to obtain short-circuit current measurements and assessment of functional microanatomy. A minimum of 5 wells were tested per condition. Human sinonasal epithelial cells cultured from a patient negative for mutations in the CFTR gene were seeded on glass coverslips and used for Fura-2 calcium imaging.

### 2.2. Fisher rat thyroid cells expressing human CFTR

Fisher rat thyroid (FRT) cells expressing human wild-type CFTR were received from the Gregory Fleming James Cystic Fibrosis

Research Center. cDNAs carrying human WT CFTR were introduced into FRT cells using the Flp-in system (Invitrogen, Grand Island, NY, USA). FRT cells were developed in media containing Coon's modified Ham's F-12 with 5% fetal bovine serum and 100  $\mu\text{g}/\text{mL}$  hygromycin. Cell media were substituted every 48 hours. For Ussing chamber studies,  $7.5 \times 10^4$  FRT cells were grown on 6.5mm Transwell with 0.4- $\mu\text{m}$  pore membrane inserts for 4 days. Apical and basolateral media were replaced every 48 hours.

### 2.3. Ussing chamber analysis

Cultures on filters (Costar) were inserted into Ussing chambers to investigate pharmacologic manipulation of vectorial ion transport as previously described [26,29,30]. Monolayers of all cell types were appraised under short-circuit current conditions following fluid resistance compensation using automatic voltage clamping (VCC 600; Physiologic Instruments, San Diego, CA, USA). Serosal bath solutions included (in mM) 120 NaCl, 25  $\text{NaHCO}_3$ , 3.3  $\text{KH}_2\text{PO}_4$ , 0.8  $\text{K}_2\text{HPO}_4$ , 1.2  $\text{MgCl}_2$ , 1.2  $\text{CaCl}_2$ , and 10 glucose. Baths for Transwell cultures were warmed to 37°C and gassed continuously with a 95%  $\text{O}_2$ –5%  $\text{CO}_2$  mixture that provides a pH of 7.4 under the conditions studied here. Chemicals were obtained from Sigma (St. Louis, MO, USA). RGAE was provided by the Korea Ginseng & Tobacco Central Research Institute and contains 7.9 mg/g as a sum of major ginsenosides Rb1, Rg1, and Rg3 (Table 1) [31]. Rb1, Rg1, and Rg3 were also tested and ordered separately through Sigma. Ussing chamber experiments were executed with a nominal mucosal  $\text{Cl}^-$  in which 6 mM NaCl + 114 mM Na gluconate replaced NaCl in the above solution. We used the following pharmacologic agents for these studies: amiloride (100  $\mu\text{M}$ ) — blocks epithelial  $\text{Na}^+$  channels, as a means to isolate changes in short-circuit current ( $\Delta I_{\text{SC}}$ ) due to effects on  $\text{Cl}^-$  channel activity; forskolin (20  $\mu\text{M}$ ) — activates CFTR by elevating intracellular cAMP, which causes protein kinase A–dependent phosphorylation of the CFTR regulatory domain (R-D); INH-172 (10  $\mu\text{M}$ ) — a CFTR inhibitor that allows determination of CFTR-dependent contributions to  $I_{\text{SC}}$ ; tannic acid (100 mM) — an inhibitor of CaCC; and uridine 5-triphosphate (UTP, 150  $\mu\text{M}$ ) — activates CaCC. Each solution was produced as 1,000  $\times$  stock and studied at 1  $\times$ . The  $I_{\text{SC}}$  was constantly assessed at one current measurement per second. A positive deflection in  $I_{\text{SC}}$  under conditions tested here was defined as the net movement of anions from the serosa to the mucosa.

### 2.4. Whole-cell patch clamp analysis

Mouse transmembrane protein 16A (TMEM16A) subcloned in frame within the enhanced green fluorescent protein (pEGFP)-N1 vector was provided by Professor Lily Y. Jan (University of California, San Francisco). The TMEM16A-GFP was built as previously

**Table 1**  
Composition of Korean Red Ginseng extracts

Ginsenoside	Korean Red Ginseng extracts (mg/g)
<b>Rg1</b>	<b>1.10 ± 0.07</b>
Re	1.57 ± 0.17
Rf	0.95 ± 0.01
Rh1	0.87 ± 0.09
Rg2s	1.83 ± 0.15
<b>Rb1</b>	<b>4.70 ± 0.17</b>
Rc	2.03 ± 0.15
Rb2	1.76 ± 0.15
Rd	0.67 ± 0.04
<b>Rg3s</b>	<b>2.13 ± 0.05</b>
Rg3r	0.83 ± 0.02
	7.9 mg/g

The three major ginsenosides (Rg1, Rb1, and Rg3) in Korean RGAE are marked in bold characters.

described by Schroeder et al. [32]. Human embryonic kidney (HEK) 293 cells were transfected using Lipofectamine 2000 Transfection reagent (Cat. No: 11668; Life technologies, Carlsbad, Ca, USA) according to the manufacturer's instructions. Stably TMEM16A-transfected HEK 293 cells were maintained in Dulbecco's Modified Eagle's medium supplemented with 10% fetal bovine serum and 0.4 mg/mL G418 at 37°C in 5% CO<sub>2</sub> and passaged every 2–5 d. Cells were split and seeded on glass coverslips one day before whole-cell patch clamp analysis. Each cover slip with cells was transferred to an experimental chamber mounted on the stage of an Olympus microscope. TMEM16A currents were recorded in whole-cell mode of the patch clamp technique using an Axopatch 2000B amplifier interfaced through DIGITA 1440A to a computer. The data were recorded and examined using the pClamp 10.6 software (Molecular Devices, San Jose, Ca, USA). During the experiments, cells were perfused with an external solution of the following ionic composition (in mM): 145 CsCl, 2 MgCl<sub>2</sub>, 2 CaCl<sub>2</sub>, 5.5 Glucose, 10 HEPES pH 7.4 (1 N NaOH). The pipette resistance used for whole recording ranged from 3 to 5 GV when filled with the intrapipette solution (in mM): 135 CsCl, 10 KCl, 2 MgCl<sub>2</sub>, 0.1 EGTA, 5.5 Glucose, 10 HEPES, pH 7.2 (1N KOH). All experiments were achieved at room temperature. Cells were continuously perfused with the external solution until formation of the recording whole cell configuration. Activators of

TMEM16A were applied through the same perfusion system. The rate of perfusion was adjusted to 1 mL/min. The data were analyzed and plotted using Igor Pro. 8 (Wavemetrics, Lake Oswego, OR, USA).

### 2.5. Micro-optical coherence tomography imaging

To assess the functional microanatomy parameters of ASL depth and ciliary beat frequency (CBF), micro-optical coherence tomography ( $\mu$ OCT) imaging of MNSE cultures was performed with incident illumination of the apical cell surface. To mitigate errors in geometric measurements, the imaging optics axis was placed within 10 degrees of normal to the cell plane as previously described [33,34]. All imaging was performed at 4 regions of interest per each well (2 points at 1 mm from the center and another at 1 mm from the edge for 2 separate locations). ASL was quantitatively evaluated by directly gauging the visible thickness of the respective layers in the image. To account for refractory properties of the liquid, layer thickness dimensions were corrected for the index of refraction of the liquid ( $n = 1.33$ ). CBF was calculated using a time series of images and quantitatively measured by identifying peak amplitude frequency in the temporal Fourier transform of areas demonstrating oscillatory behavior [33]. All parameters were judged at 5 uniformly distributed areas of the image. All images

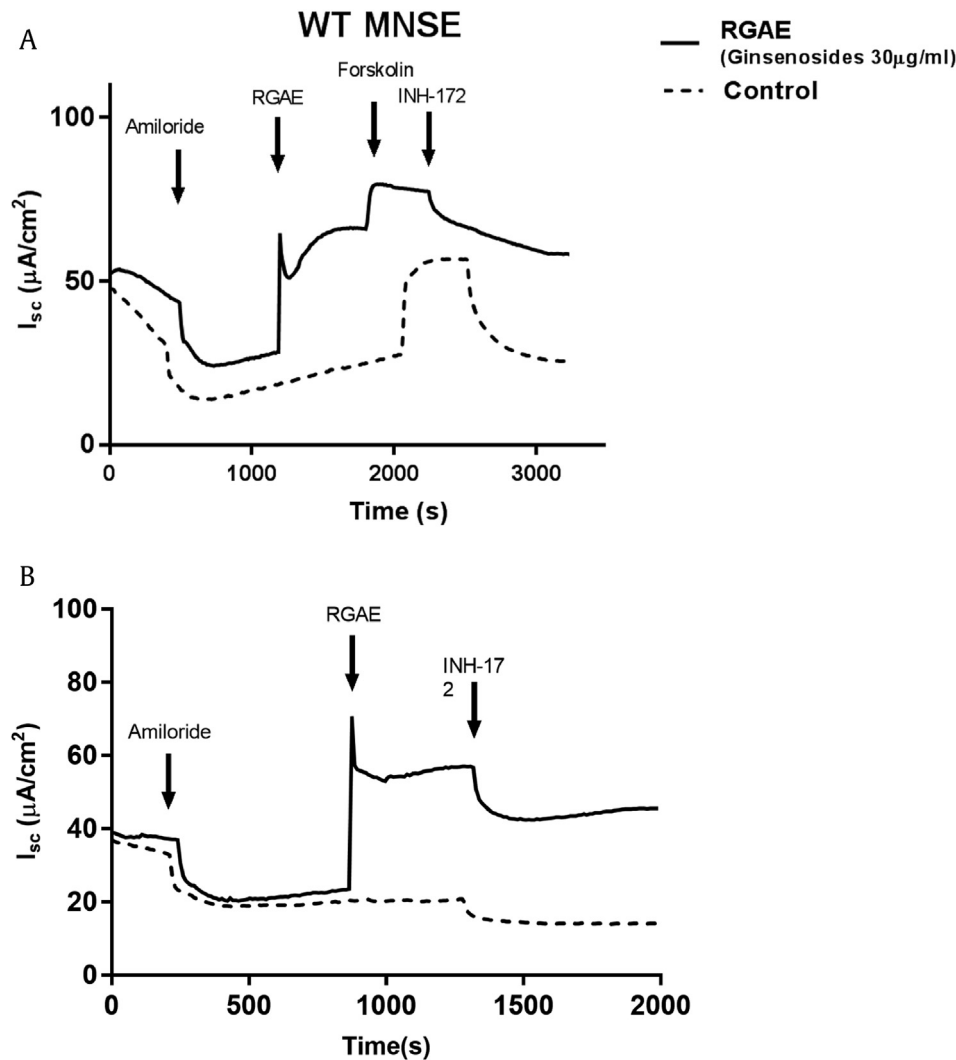


**Fig. 1. Representative Ussing chamber tracings.** Representative Ussing chamber tracings demonstrate pharmacologic manipulation of ion transport with activation of Cl<sup>-</sup> secretion in murine nasal septal epithelial (MNSE, wild type [WT]) cell cultures with RGAE followed by forskolin and INH-172 (Fig. 1A) vs RGAE followed by INH-172 (Fig. 1B). MNSE, murine nasal septal epithelial; RGAE, red ginseng aqueous extract;  $I_{sc}$ , short circuit current.

were analyzed utilizing ImageJ version 1.50i (National Institutes of Health, Bethesda, MD, USA) and MATLAB® R2016a (The MathWorks, Natick, MA, USA).

## 2.6. Fura-2 imaging

Human sinonasal epithelial cells seeded on a glass coverslip were loaded with the  $\text{Ca}^{2+}$ -sensitive dye Fura-2, and changes in cytosolic calcium  $[\text{Ca}^{2+}]_i$  measured with dual excitation wavelength fluorescence microscopy [2]. Cells were sequentially perfused with solutions containing RGAE or vehicle control, followed by 140 mM UTP (Sigma) as a positive control. Fluorescence intensity was monitored by a Photon Technology International (Birmingham, NJ) dual wavelength spectrofluorometer (excitation wavelength: 340/380 nm and emission wavelength: 510 nm). The intensity of fluorescence was calculated automatically. The  $R_{\text{max}}$  and  $R_{\text{min}}$  values were calculated by the addition of 3 mM  $\text{Ca}^{2+}$  and 5 mM EGTA plus 5  $\mu\text{M}$  ionomycin, respectively.

## 2.7. Statistical analysis

Statistical analyses were conducted with Excel 2016 and GraphPad Prism 6.0 software (La Jolla, Ca) using an unpaired t-test

or subgroup one-way ANOVA with post hoc Tukey's test with significance set at  $P < 0.05$  centered on the characteristics of comparison.

## 3. Results

### 3.1. RGAE increases transepithelial $\text{Cl}^-$ transport in WT primary MNSE

To evaluate the impact of RGAE on transepithelial anion transport, cell cultures were mounted in Ussing chambers for measurements of short circuit current ( $I_{\text{SC}}$ ) using pharmacologic manipulation. After blocking epithelial sodium channels with amiloride, RGAE-dependent  $\Delta I_{\text{SC}}$  (in  $\text{mA}/\text{cm}^2$ ) was tested in WT MNSE (Fig. 1). Summary data are presented in Fig. 2A ( $n = 6$ , each group). RGAE (at  $30\mu\text{g}/\text{mL}$  of ginsenosides) significantly increased  $\Delta I_{\text{SC}}$  when compared with vehicle control in WT MNSE (RGAE vs Control =  $49.8 \pm 2.6$  vs  $0.1 \pm 0.2$ ,  $p < 0.0001$ ). Interestingly, the  $\Delta I_{\text{SC}}$  by RGAE ( $30\mu\text{g}/\text{mL}$  of ginsenosides) was significantly higher than  $\Delta I_{\text{SC}}$  amplified by forskolin, which maximally activates CFTR-mediated anion secretion ( $\Delta I_{\text{SC}} = 33.9 \pm 2.2 \text{ mA}/\text{cm}^2$ ,  $p < 0.001$ ). The RGAE-mediated  $\text{Cl}^-$  secretion in WT MNSE was dose-dependent (Fig. 2B). INH-172 (an inhibitor of CFTR) was also

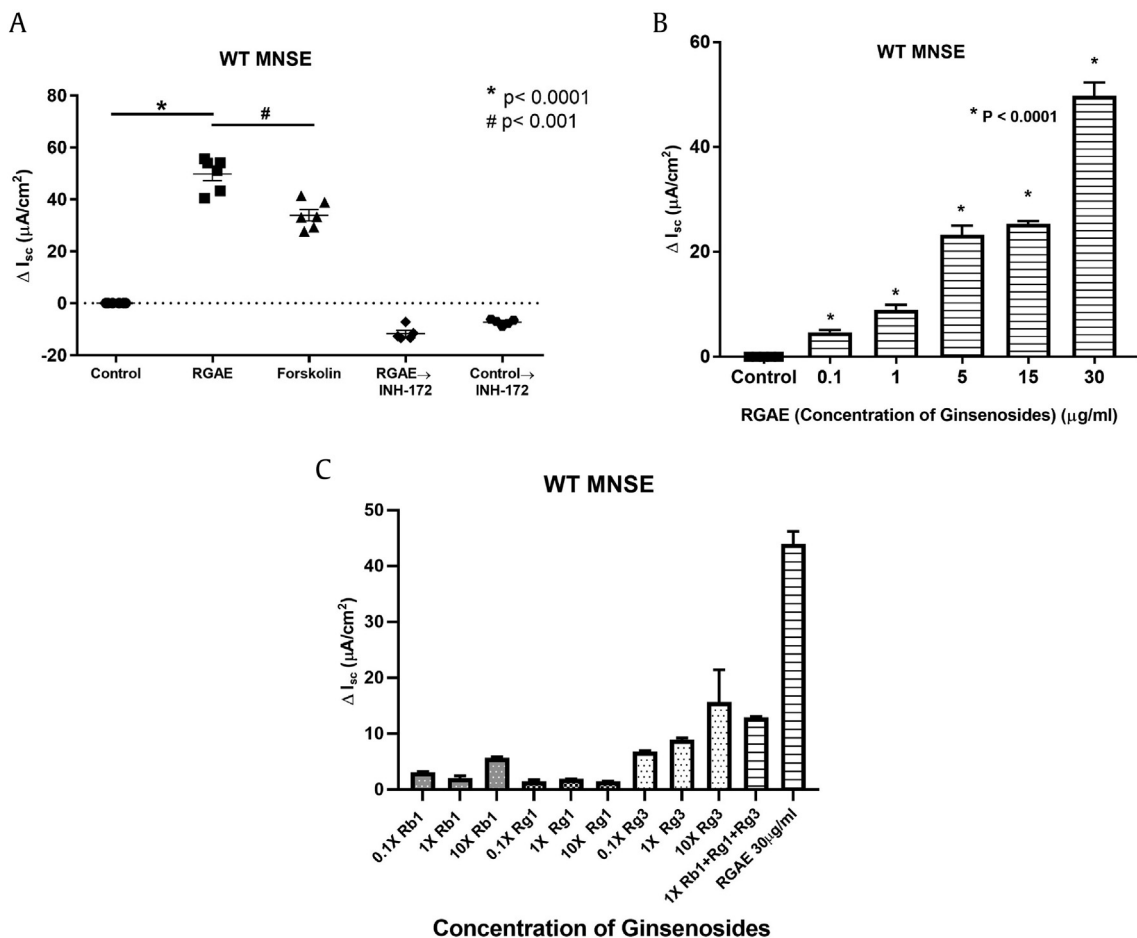


**Fig. 2. Summary data for RGAE-stimulated  $\Delta I_{\text{SC}}$  in WT MNSE.** A. RGAE (at  $30\mu\text{g}/\text{mL}$  of Ginsenosides) significantly increased  $\Delta I_{\text{SC}}$  when compared with control in WT MNSE (WT vs control =  $49.8 \pm 2.6$  vs  $0.0 \pm 0.0$ ,  $p < 0.0001$ ). In WT MNSE, the  $\Delta I_{\text{SC}}$  by RGAE was significantly higher than  $\Delta I_{\text{SC}}$  amplified by forskolin ( $\Delta I_{\text{SC}} = 33.9 \pm 2.2 \text{ mA}/\text{cm}^2$ ,  $p < 0.001$ ). INH-172 significantly blocked  $\Delta I_{\text{SC}}$  that was generated by RGAE compared with control (RGAE + INH-172 vs Control + INH-172 =  $-11.7 \pm 1.2$  vs  $-7.3 \pm 0.5$ ,  $p < 0.01$ ). \*:  $p < 0.0001$ , #:  $p < 0.001$ . B. Dose-dependent  $\text{Cl}^-$  secretion was observed with escalating concentrations of RGAE ( $n = 6$ ). C. Dose-response of individual ginsenosides Rb1, Rg1, and Rg3 in WT MNSE. Rg3 was the most robust activator at a dose consistent with the concentration in RGAE used in this study. Total  $I_{\text{SC}}$  using all 3 components only activated approximately 30% of total  $I_{\text{SC}}$  with RGAE (Rb1 + Rg1 + Rg3 vs RGAE =  $12.9 \pm 0.14$  vs  $44.0 \pm 2.21$ ,  $p < 0.0001$ ). \* represents significance compared with the control group ( $p < 0.0001$ ). MNSE, murine nasal septal epithelial; RGAE, red ginseng aqueous extract;  $I_{\text{SC}}$ , short circuit current; WT, wild type.

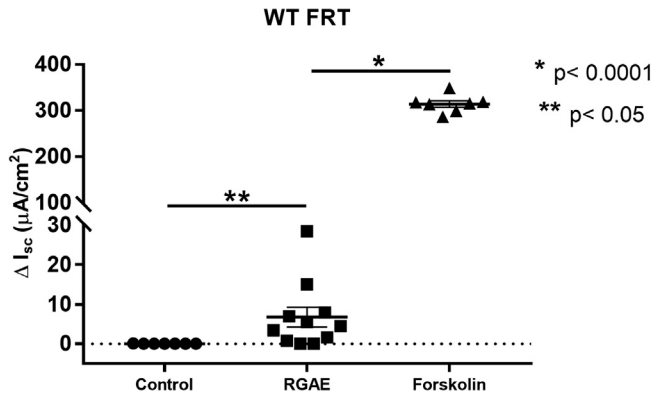


**Fig. 3. Summary Data for RGAE-stimulated  $\Delta I_{sc}$  in FRT cells expressing human WT CFTR.** FRT cells expressing human WT CFTR were used to stimulate RGAE. Exposure to RGAE (30  $\mu\text{g}/\text{mL}$  of Ginsenosides) resulted in a small but statistically significant increase in  $\Delta I_{sc}$  (RGAE vs Control =  $6.8 \pm 2.5$  vs  $0.03 \pm 0.01$ ,  $p = 0.024$ ). \*:  $p < 0.0001$ . CFTR, cystic fibrosis transmembrane conductance regulator; FRT, fisher rat thyroid; RGAE, red ginseng aqueous extract;  $I_{sc}$ , short circuit current; WT, wild type.

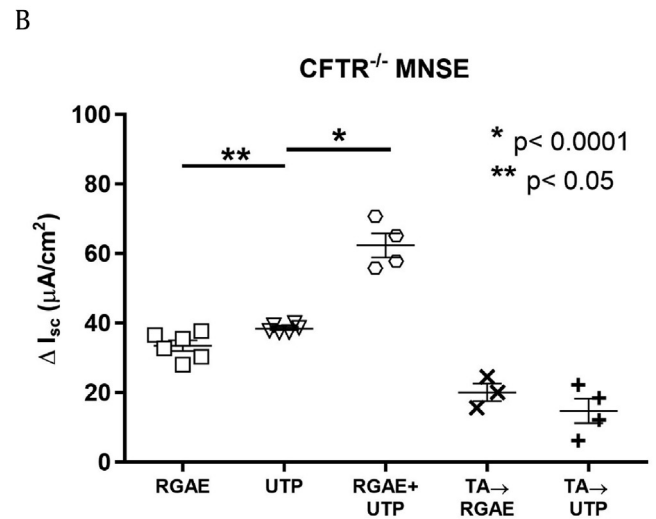
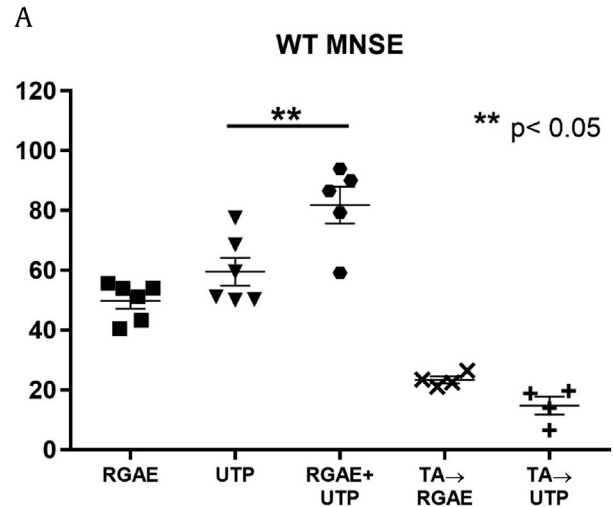


**Fig. 5. Summary data for CaCC-mediated chloride secretion by RGAE in WT and  $CFTR^{-/-}$  MNSE.** The maximum capability for vectorial  $\text{Cl}^{-}$  transport was significantly improved with both agents (RGAE and UTP) compared with UTP alone in both WT (A) and  $CFTR^{-/-}$  MNSE (B) (WT MNSE: RGAE + UTP =  $81.8 \pm 6.2$  vs UTP =  $59.5 \pm 4.7$ ,  $p < 0.05$ ;  $CFTR^{-/-}$  MNSE: RGAE + UTP =  $62.3 \pm 3.4$  vs UTP =  $38.4 \pm 0.5$ ,  $p < 0.01$ ), indicating that RGAE improves the UTP response. The addition of the tannic acid partly (about 50%) reduced the RGAE-evoked increase in both types of MNSE (WT MNSE from  $49.8 \pm 2.6$   $\mu\text{A}/\text{cm}^2$  to  $23.3 \pm 1.1$   $\mu\text{A}/\text{cm}^2$ ,  $P < 0.0001$ ;  $CFTR^{-/-}$  MNSE from  $33.5 \pm 1.5$   $\mu\text{A}/\text{cm}^2$  to  $20.1 \pm 2.6$   $\mu\text{A}/\text{cm}^2$ ,  $P < 0.05$ , Fig. 5A and B). CaCC, calcium-activated chloride channel; CFTR, cystic fibrosis transmembrane conductance regulator; MNSE, murine nasal septal epithelial; RGAE, red ginseng aqueous extract;  $I_{sc}$ , short circuit current; UTP, uridine 5-triphosphate; WT, wild type.

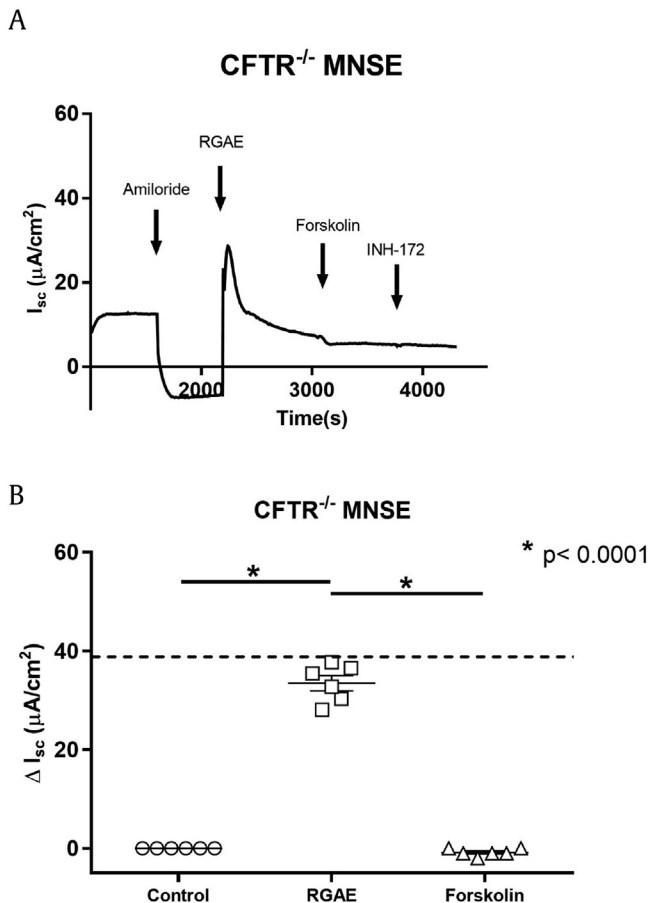


**Fig. 4. Representative Ussing chamber tracings and summary data for RGAE-stimulated  $\Delta I_{sc}$  in  $CFTR^{-/-}$  MNSE.** A. A representative Ussing chamber tracing demonstrates activation of  $\text{Cl}^{-}$  secretion in  $CFTR^{-/-}$  MNSE cells following blockade of epithelial sodium channels by amiloride. B. RGAE (at 30  $\mu\text{g}/\text{mL}$  of ginsenosides) significantly increased  $\Delta I_{sc}$  when compared with control in  $CFTR^{-/-}$  MNSE ( $CFTR^{-/-}$  =  $33.5 \pm 1.5$  vs  $0.0 \pm 0.0$ ,  $p < 0.0001$ ). RGAE-dependent  $\Delta I_{sc}$  in  $CFTR^{-/-}$  MNSE was similar to forskolin-mediated  $\Delta I_{sc}$  in WT MNSE (dotted line) ( $p = 0.87$ ) ( $n = 6$ ). \*:  $p < 0.0001$ . CFTR, cystic fibrosis transmembrane conductance regulator; RGAE, red ginseng aqueous extract;  $I_{sc}$ , short circuit current; WT, wild type.

added to the mucosal bathing solution after stimulating the cells either with RGAE or control (saline) (Fig. 1B) to understand the contribution of CFTR-mediated  $\text{Cl}^{-}$  secretion. In RGAE stimulated cultures, INH-172 only partially inhibited  $I_{sc}$ , although still significantly greater than controls (RGAE  $\rightarrow$  INH-172 vs Control  $\rightarrow$  INH-172 =  $-11.7 \pm 1.2$  vs  $-7.3 \pm 0.5$ ,  $p < 0.01$ ) (Fig. 2A). When individual ginsenosides were tested in WT MNSE, Rg3 appeared to generate the most  $\text{Cl}^{-}$  transport at a concentration (11.23  $\mu\text{g}/\text{mL}$ ) present in 30  $\mu\text{g}/\text{mL}$  of RGAE. When Rb1, Rg1, and Rg3 were tested together at doses that comprise 30  $\mu\text{g}/\text{mL}$  of RGAE,  $\Delta I_{sc}$  was approximately 30% of total  $I_{sc}$  generated with RGAE indicating other untested components also contribute to activation of CaCCs (Fig. 2C). Based on this experiment, RGAE-stimulated  $\text{Cl}^{-}$  secretion is only minimally mediated through CFTR. To better assess the impact on CFTR-

mediated anion secretion in cells that lack CaCCs, FRT cells expressing human WT CFTR were evaluated in the Ussing chamber (Fig. 3). Exposure to RGAE (30 $\mu$ g/mL of Ginsenosides) resulted in a small but statistically significant increase in  $\Delta I_{SC}$  (RGAE vs Control =  $6.8 \pm 2.5$  vs  $0.03 \pm 0.01$ ,  $p = 0.024$ ), confirming that CFTR contributes minimally to RGAE-mediated  $Cl^-$  secretion.

### 3.2. RGAE increases transepithelial $Cl^-$ transport in CFTR $^{-/-}$ primary MNSE

Primary CFTR $^{-/-}$  MNSE cultures were utilized to eliminate the contribution of CFTR to RGAE-dependent  $Cl^-$  transport. (Fig. 4A). Summary data are presented in Fig. 4B. RGAE (at 30 $\mu$ g/mL of Ginsenosides) significantly increased  $\Delta I_{SC}$  when compared with vehicle control in CFTR $^{-/-}$  MNSE (CFTR $^{-/-}$  =  $33.5 \pm 1.5$  vs  $0.2 \pm 0.3$ ,  $p < 0.0001$ ). RGAE- (30 $\mu$ g/mL of Ginsenosides) dependent  $\Delta I_{SC}$  in CFTR $^{-/-}$  MNSE ( $\Delta I_{SC} = 33.5 \pm 1.5$  mA/cm $^2$ ) was similar to forskolin-mediated  $\Delta I_{SC}$  in WT MNSE (dotted line in Fig. 4B), suggesting the magnitude of  $I_{SC}$  stimulation by RGAE achieves a range that could confer potential therapeutic benefit, particularly in patients with CF or otherwise dysfunctional CFTR.

### 3.3. CaCC-mediated chloride secretion by RGAE

To understand the impact of RGAE on transepithelial anion transport via CaCC, in some conditions, tannic acid (a non-selective CaCC blocker) was added to the mucosal and serosal bathing solution 10 min before the application of RGAE and/or UTP in WT MNSE (Fig. 5A) and CFTR $^{-/-}$  MNSE (Fig. 5B). In the absence of tannic acid, the maximum capability for vectorial  $Cl^-$  transport was significantly improved with both agents (RGAE and UTP) compared with UTP alone in both WT and CFTR $^{-/-}$  MNSE (WT MNSE: RGAE + UTP =  $81.8 \pm 6.2$  vs UTP =  $59.5 \pm 4.7$ ,  $p < 0.05$ ; CFTR $^{-/-}$  MNSE:

RGAE + UTP =  $62.3 \pm 3.4$  vs UTP =  $38.4 \pm 0.5$ ,  $p < 0.01$ ), indicating that RGAE partially potentiates the UTP response. Tannic acid partly reduced the RGAE-evoked increase in both epithelia by approximately 50% (WT MNSE from  $49.8 \pm 2.6$   $\mu$ A/cm $^2$  to  $23.3 \pm 1.1$   $\mu$ A/cm $^2$ ,  $P < 0.0001$ ; CFTR $^{-/-}$  MNSE from  $33.5 \pm 1.5$   $\mu$ A/cm $^2$  to  $20.1 \pm 2.6$   $\mu$ A/cm $^2$ ,  $P < 0.05$ , Fig. 5A and B). These results revealed that CaCC is responsible for at least 50% of RGAE-induced  $Cl^-$  transport.

### 3.4. RGAE potentiates the UTP-induced $Cl^-$ secretion as judged by whole-cell patch clamp analysis

TMEM16A, a member of a family of putative plasma membrane proteins, has been identified as a CaCC [6]. Stable, recombinant HEK293 cell line expressing human TMEM16A (also called anoctamin 1 [ANO1]) was used to activate TMEM16A by RGAE in the whole-cell patch clamp current assay. TMEM16A activity is markedly enhanced with UTP as expected (Fig. 6A). However, RGAE minimally activated TMEM16A currents when UTP was not present. TMEM16A-mediated currents at 100 mV ( $n = 12$ ) were markedly improved with co-administration of RGAE and UTP ( $8406.3 \pm 807.7$  pA) over UTP ( $3524.1 \pm 292.4$  pA) or RGAE alone ( $465.2 \pm 90.7$  pA) (Fig. 6,  $p < 0.001$ ). Patch clamp technique controls the membrane potential of the cell better than Ussing chamber technique and demonstrates that the current related to combined application (in presence of UTP) was greater than the sum of the individual currents from either agent alone, indicating synergism.

### 3.5. RGAE enhances ASL depth and CBF using $\mu$ OCT

It is well established that promoting transepithelial  $Cl^-$  secretion leads to airway surface hydration and promotes ASL depth. To evaluate effects of the formulation on ASL, WT MNSE cultures were exposed to RGAE (30 $\mu$ g/mL of ginsenosides) for 4 hours at the

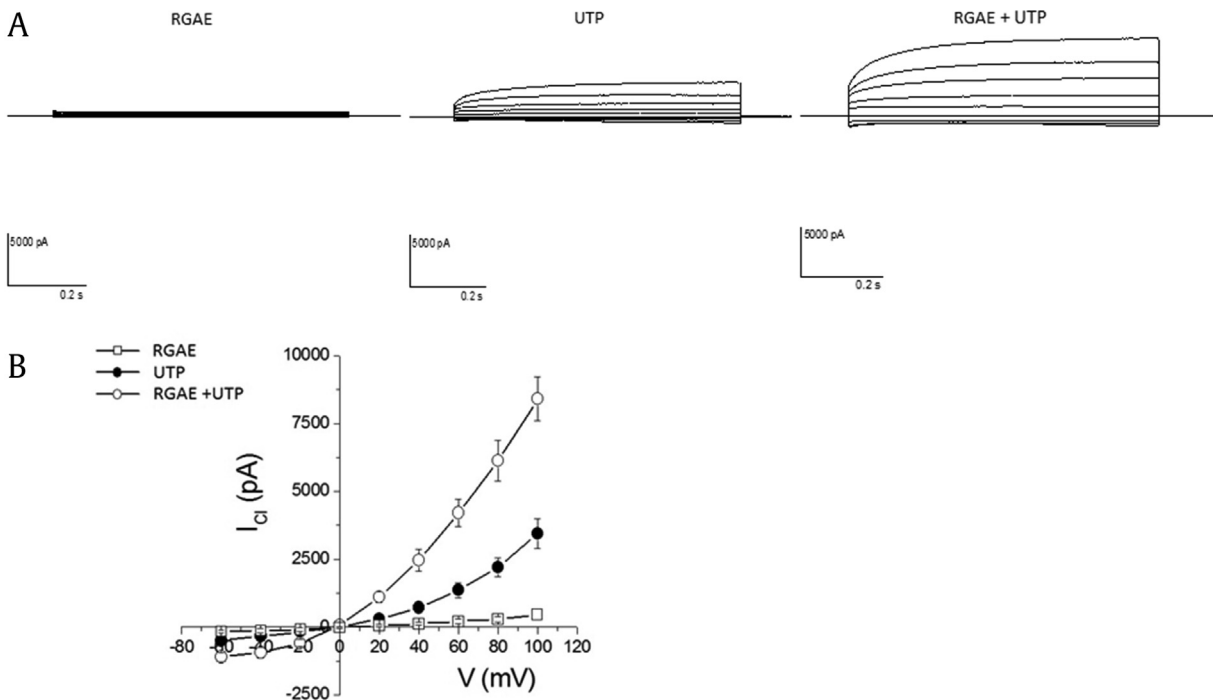


**Fig. 6. Activation currents in TMEM16A stably transfected HEK cells in whole-cell patch clamp recordings.** A. Increasing activation currents induced by RGAE, UTP, and RGAE + UTP. B. IV curves are illustrated during the activation of the  $Cl^-$  current with RGAE, UTP, and RGAE + UTP when voltage steps were varied from  $-60$  to  $100$  mV in  $20$  mV increments. The cell membrane potential was held at  $0$  mV throughout the experiment. HEK, human embryonic kidney; RGAE, red ginseng aqueous extract; TMEM16A, transmembrane protein 16A; UTP, uridine 5-triphosphate.

basolateral side and  $\mu$ OCT was used to assess ASL depth and CBF (n = 6; Fig. 7A). Mean ASL was significantly greater in the RGAE group compared with the vehicle control group (RGAE:  $6.2 \pm 0.3 \mu\text{m}$  vs Control:  $3.9 \pm 0.09 \mu\text{m}$ ,  $p < 0.0001$ ) (Fig. 7B). When cultures were exposed to RGAE for 4 hours, mean CBF was also significantly faster in RGAE exposed cells than controls ( $10.4 \pm 0.3 \text{ Hz}$  vs  $7.3 \pm 0.2 \text{ Hz}$ ;  $p < 0.0001$ ).

### 3.6. RGAE did not alter $[\text{Ca}^{2+}]_i$ at concentrations consistent with CaCC activation

Because RGAE is a dark brown liquid, at higher concentrations we were unable to evaluate  $[\text{Ca}^{2+}]_i$  fluctuations due to the diminished fluorescence present from coloration of the solution. RGAE at  $1 \mu\text{g}/\text{mL}$  was the maximum dose by which  $[\text{Ca}^{2+}]_i$  could be assessed and was previously confirmed to significantly increase  $\Delta I_{\text{SC}}$ . Fluorescence measurements confirmed no alteration in  $[\text{Ca}^{2+}]_i$ , while

positive control (UTP) caused robust release of intracellular  $[\text{Ca}^{2+}]_i$  stores (Fig. 8 — an experiment performed in triplicate).

## 4. Discussion

Korean Red Ginseng (*P. ginseng Meyer*) is widely used as an alternative medicine and health-enhancing supplement [31]. Approximately 8,000 tons of ginseng is produced per year and consumed around the world because of its ostensible immune boosting functions and antimicrobial activity [35,36]. *P. ginseng* is classified as either an herbal medicine or a health food supplement depending on the country where it is sold [20].

In the present study, application of the bioactive components of ginseng to the surface of WT MNSE stimulated  $\text{Cl}^-$  secretion in a sustained fashion and was higher than maximally stimulated CFTR-mediated anion secretion by forskolin. TMEM16A-mediated chloride currents were markedly improved with co-administration with UTP. Markers of functional microanatomy (ASL and CBF) that

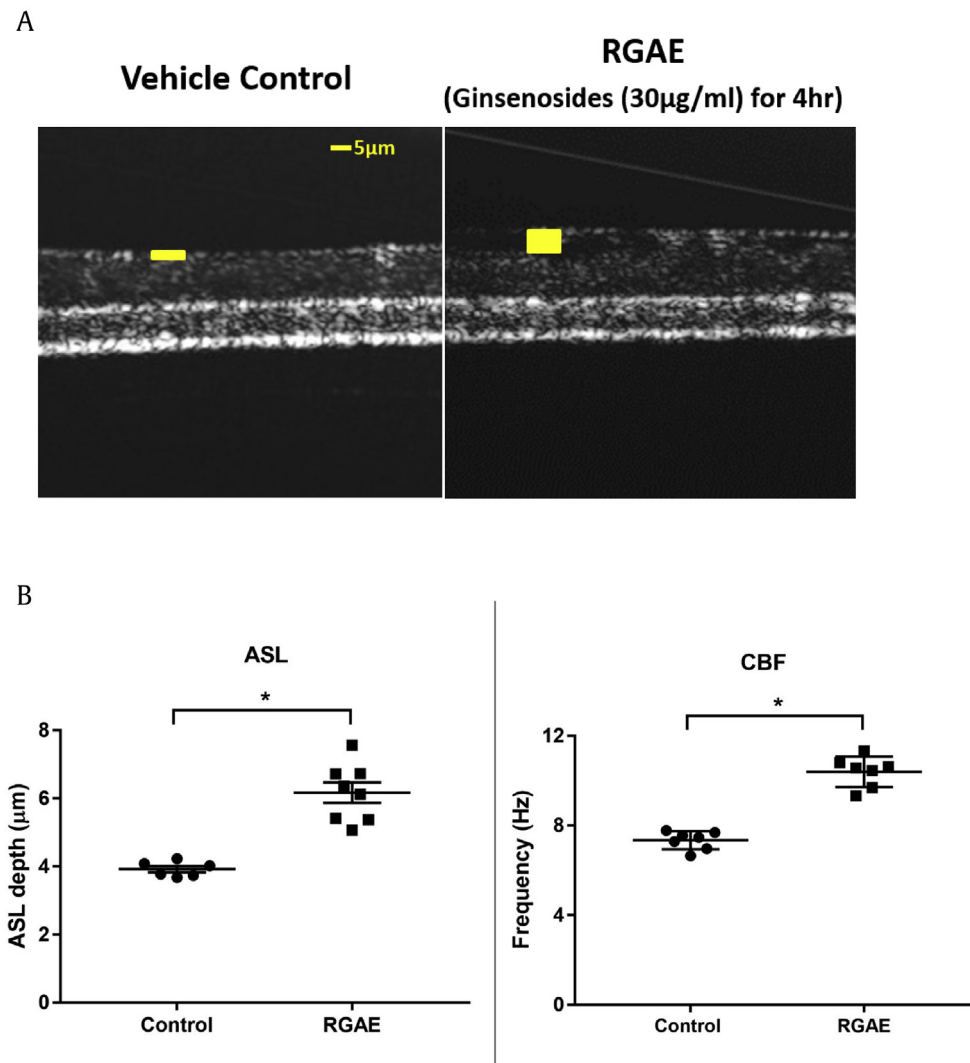


**Fig. 7. Measurement of ASL depth using  $\mu$ OCT.** A.  $\mu$ OCT images demonstrating ASL thickness in control (A) and RGAE-stimulated (B) MNSE cell cultures. Yellow bar = ASL depth. Scale bar = 5  $\mu\text{m}$ . B. Mean ASL was significantly greater in the RGAE group when compared with the vehicle control group (RGAE:  $6.2 \pm 0.3 \mu\text{m}$  vs Control:  $3.9 \pm 0.09 \mu\text{m}$ ,  $*$ ;  $p < 0.0001$ ). The mean CBF was also significantly faster in RGAE exposed cells compared with controls ( $10.4 \pm 0.3 \text{ Hz}$  vs  $7.3 \pm 0.2 \text{ Hz}$ ;  $p < 0.0001$ ). All groups consisted of at least six experiments with monolayer per condition.

ASL, airway surface liquid;  $\mu$ OCT, micro-optical coherence tomography; RGAE, red ginseng aqueous extract; CBF, ciliary beat frequency.

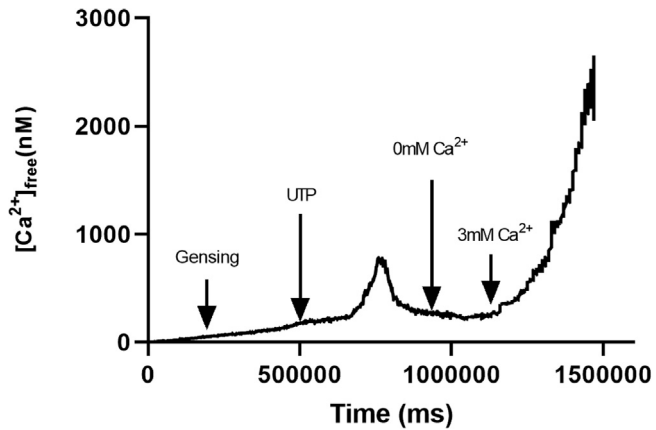


**Fig. 8.** Fura-2  $[Ca^{2+}]_i$  imaging. Representative Fura-2 fluorescence curve demonstrating no release of  $[Ca^{2+}]_i$  at a dose of RGAE (1  $\mu\text{g}/\text{mL}$ ) shown to stimulate trans-epithelial  $Cl^-$  secretion.

are influenced by apical  $Cl^-$  secretion were also enhanced with exposure to RGAE. Importantly, RGAE-mediated  $Cl^-$  transport in CFTR<sup>-/-</sup> MNSE was also robust despite the absence of CFTR channel function and was similar to forskolin-induced  $Cl^-$  secretion in WT MNSE, indicating currents were largely independent of CFTR. Indeed RGAE-dependent  $Cl^-$  secretion in CFTR<sup>-/-</sup> MNSE was approximately 30% less than the  $\Delta I_{SC}$  observed in WT MNSE. However, CFTR is also partially activated via elevation of cytosolic  $Ca^{2+}$ , and therefore this may not be attributable to direct activation of CFTR by RGAE [37]. To understand the direct contribution of CFTR-mediated  $Cl^-$  secretion when stimulated with RGAE, we used a CFTR-specific blocker (CFTR<sub>inh</sub>-172) and FRT cells expressing CFTR. Based on these analyses (Figs. 2 and 3), the direct contribution of CFTR-mediated  $Cl^-$  secretion to RGAE-dependent  $\Delta I_{SC}$  appears to be minimal (less than 10%). Therefore, the transepithelial  $Cl^-$  transport observed in CFTR<sup>-/-</sup> MNSE indicates alternative  $Cl^-$  channels (such as CaCC) are primarily responsible for RGAE-stimulated  $Cl^-$  transport. As the maximum capability for vectorial  $Cl^-$  transport was significantly improved with both agents (RGAE and UTP) compared with UTP alone in CFTR<sup>-/-</sup> MNSE (Fig. 5B), other  $Cl^-$  channels (such as SLC26A9) may also be responsible for RGAE-stimulated  $Cl^-$  transport or RGAE could serve as a potentiator of UTP.

Activators of TMEM16A (a voltage sensitive CaCC) are capable of stimulating anion transport and improve mucin release from goblet cells, as well as promoting MCC [18]. The role of TMEM16A in the airway surface epithelium remains controversial, but increased TMEM16A-CaCC channel abundance and activity might contribute to mucus secretion and airway hyper-responsiveness in asthmatics [38]. Guo et al has previously demonstrated that TMEM16 was directly activated by ginsenoside Rb1 causing increased contraction of guinea pig intestine [22]. The aqueous extract used in the present study contains multiple ginsenosides including Rb1 (Table 1) and the doses used in the experiments by Guo et al. (100 $\mu\text{M}$  of Rb1) were much higher (x 5.6) than our maximum concentration. When testing individual ginsenosides, Rb1 was tested at a ten-fold concentration and was observed to have minimal impact on trans-epithelial  $Cl^-$  secretion. Rg3 appears to be the most active of the ginsenosides, however, even with combining all 3 ginsenosides (Rb1, Rg1, and Rg3), these were only capable of stimulating approximately 30% of the RGAE-stimulated  $Cl^-$  transport. Thus, other constituents in RGAE that have yet to be described may contribute to the robust stimulation of  $Cl^-$  secretion.

Gintonin is one such component identified in RGAE that has been previously shown to activate CaCC in mammalian cells through G-protein-coupled lysophosphatidic acid receptor

signaling pathways, primarily through driving intracellular  $[Ca^{2+}]_i$  [39]. Gintonin is a glycolipoprotein fraction from a crude ginseng total saponin. It is a complex of lysophosphatidic acid and ginseng proteins such as ginseng major latex-like protein 151 (GLP151) and ginseng ribonuclease-like storage protein. Based on a study by Choi et al. [40], the amount of gintonin extracted from the ginseng root is extremely small after considering all the loss during purification. While this could activate CaCC transport, its direct effect from the RGAE is likely negligible. Standard purified gintonin is not available, which makes it problematic to perform any *in vitro* test.

In whole-cell patch-clamp experiments, RGAE minimally stimulated TMEM16A alone but led to synergistically increased  $I_{SC}$  when combined with UTP over UTP alone, suggesting RGAE may not affect  $[Ca^{2+}]_i$  release or  $[Ca^{2+}]_i$  entry through activation of CaCCs. This is supported by Fura-2 imaging data showing no changes in  $[Ca^{2+}]_i$  at an RGAE concentration (1 $\mu\text{g}/\text{mL}$ ) capable of stimulating  $Cl^-$  secretion. However, RGAE may affect the expression of TMEM16A at the membrane or its channel conductance, or both. Previous studies have demonstrated that RGAE reduced the nasal allergic inflammatory reaction in allergic rhinitis and countered asthmatic effects in ovalbumin-induced asthma model in mice. Thus, RGAE may not increase airway hyper-responsiveness, commonly seen in allergic airway diseases, but rather facilitate MCC by hydrating ASL. Further studies are required to establish the underlying mechanism of RGAE in airway epithelial cells.

There are several limitations to this study. This is an *in vitro* investigation, and the drug was not tested in *in vivo* animal models. Previously published work using CFTR<sup>-/-</sup> mice demonstrated only a mild pathology, which was in opposition to the observed disease in humans, and this may be due to substantial amounts of CaCC anion secretion in mice [41,42]. Further studies will include evaluation in human sinonasal or bronchial cells *in vitro* and *ex vivo* and assessment of RGAE-mediated effects on CF murine and rat animal models [43,44].

## 5. Conclusion

RGAE stimulated  $Cl^-$  secretion in a sustained fashion in both WT and CFTR<sup>-/-</sup> MNSE and augments both ASL depth and CBF. These findings suggest RGAE has therapeutic potential for both CF and non-CF chronic airway diseases, such as chronic rhinosinusitis.

## Conflicts of interest

Do-Yeon Cho, MD receives research grant support from Bionorica Inc. and Bradford A. Woodworth, M.D. is a consultant for Olympus and Cook Medical. He also receives grant support from Cook Medical and Bionorica Inc.

## Acknowledgements

This work was supported by National Institutes of Health (NIH)/ National Heart, Lung, and Blood Institute (1 R01 HL133006-04) and National Institute of Diabetes and Digestive and Kidney Diseases (5P30DK072482-05) to S.M.R. and John W. Kirklín Research and Education Foundation Fellowship Award, UAB Faculty Development Research Award, American Rhinologic Society New Investigator Award, and Cystic Fibrosis Foundation Research Development Pilot grant (ROWE15R0) to D.-Y.C.



## References

- [1] Cohen NA. Sinonasal mucociliary clearance in health and disease. *Ann Otol Rhinol Laryngol Suppl* 2006;196:20–6.
- [2] Zhang S, Skinner D, Hicks SB, Bevensen MO, Sorscher EJ, Lazrak A, Matalon S, McNicholas CM, Woodworth BA. Sinupret activates CFTR and TMEM16A-dependent transepithelial chloride transport and improves indicators of mucociliary clearance. *PLoS One* 2014;9(8):e104090.
- [3] Cho DY, Nayak JV, Bravo DT, Le W, Nguyen A, Edward JA, Hwang PH, Illek B, Fischer H. Expression of dual oxidases and secreted cytokines in chronic rhinosinusitis. *Int Forum Allergy Rhinol* 2013;3(5):376–83.
- [4] Matsui H, Randell SH, Peretti SW, Davis CW, Boucher RC. Coordinated clearance of periciliary liquid and mucus from airway surfaces. *J Clin Invest* 1998;102(6):1125–31.
- [5] Wanner A, Salathe M, O'Riordan TG. Mucociliary clearance in the airways. *Am J Respir Crit Care Med* 1996;154(6 Pt 1):1868–902.
- [6] Caputo A, Caci E, Ferrera L, Pedemonte N, Barsanti C, Sondo E, Pfeiffer U, Ravazzolo R, Zegarra-Moran O, Galiotta LJ. TMEM16A, a membrane protein associated with calcium-dependent chloride channel activity. *Science* 2008;322(5901):590–4.
- [7] Cho DY, Hwang PH, Illek B. Effect of L-ascorbate on chloride transport in freshly excised sinonasal epithelia. *Am J Rhinol Allergy* 2009;23(3):294–9.
- [8] Dransfield MT, Wilhelm AM, Flanagan B, Courville C, Tidwell SL, Raju SV, Gagar A, Steele C, Tang LP, Liu B, et al. Acquired cystic fibrosis transmembrane conductance regulator dysfunction in the lower airways in COPD. *Chest* 2013;144(2):498–506.
- [9] Rab A, Rowe SM, Raju SV, Bebok Z, Matalon S, Collawn JF. Cigarette smoke and CFTR: implications in the pathogenesis of COPD. *Am J Physiol Lung Cell Mol Physiol* 2013;305(8):L530–41.
- [10] Raju SV, Lin VY, Liu L, McNicholas CM, Karki S, Sloane PA, Tang L, Jackson PL, Wang W, Wilson L, et al. The cystic fibrosis transmembrane conductance regulator potentiator ivacaftor augments mucociliary clearance abrogating cystic fibrosis transmembrane conductance regulator inhibition by cigarette smoke. *Am J Respir Cell Mol Biol* 2017;56(1):99–108.
- [11] Solomon GM, Fu L, Rowe SM, Collawn JF. The therapeutic potential of CFTR modulators for COPD and other airway diseases. *Curr Opin Pharmacol* 2017;34:132–9.
- [12] Dey I, Shah K, Bradbury NA. Natural compounds as therapeutic agents in the treatment cystic fibrosis. *J Genet Syndr Gene Ther* 2016;7(1).
- [13] Carlile GW, Keyzers RA, Teske KA, Robert R, Williams DE, Linington RG, Gray CA, Centko RM, Yan L, Anjos SM, et al. Correction of F508del-CFTR trafficking by the sponge alkaloid latruncidine is modulated by interaction with PARP. *Chem Biol* 2012;19(10):1288–99.
- [14] Springsteel MF, Galiotta LJ, Ma T, By K, Berger GO, Yang H, Dicus CW, Choung W, Quan C, Shelat AA, et al. Benzoflavone activators of the cystic fibrosis transmembrane conductance regulator: towards a pharmacophore model for the nucleotide-binding domain. *Bioorg Med Chem* 2003;11(18):4113–20.
- [15] Galiotta LJ, Springsteel MF, Eda M, Niedzinski EJ, By K, Haddadin MJ, Kurth MJ, Nantz MH, Verkman AS. Novel CFTR chloride channel activators identified by screening of combinatorial libraries based on flavone and benzoquinolinium lead compounds. *J Biol Chem* 2001;276(23):19723–8.
- [16] Caci E, Folli C, Zegarra-Moran O, Ma T, Springsteel MF, Sammelson RE, Nantz MH, Kurth MJ, Verkman AS, Galiotta LJ. CFTR activation in human bronchial epithelial cells by novel benzoflavone and benzimidazolone compounds. *Am J Physiol Lung Cell Mol Physiol* 2003;285(1):L180–8.
- [17] Tarran R, Button B, Boucher RC. Regulation of normal and cystic fibrosis airway surface liquid volume by phasic shear stress. *Annu Rev Physiol* 2006;68:543–61.
- [18] Mall MA, Galiotta LJ. Targeting ion channels in cystic fibrosis. *J Cyst Fibros* 2015;14(5):561–70.
- [19] Lee CH, Kim JH. A review on the medicinal potentials of ginseng and ginsenosides on cardiovascular diseases. *J Ginseng Res* 2014;38(3):161–6.
- [20] Kim IW, Cha KM, Wee JJ, Ye MB, Kim SK. A new validated analytical method for the quality control of red ginseng products. *J Ginseng Res* 2013;37(4):475–82.
- [21] Kim YH, Kim GH, Shin JH, Kim KS, Lim JS. Effect of Korean red ginseng on testicular tissue injury after torsion and detorsion. *Korean J Urol* 2010;51(11):794–9.
- [22] Guo S, Chen Y, Pang C, Wang X, Qi J, Mo L, Zhang H, An H, Zhan Y. Ginsenoside Rb1, a novel activator of the TMEM16A chloride channel, augments the contraction of Guinea pig ileum. *Pflugers Arch* 2017;469(5–6):681–92.
- [23] Li L, Sheng YX, Zhang JL, Wang SS, Guo DA. High-performance liquid chromatographic assay for the active saponins from *Panax notoginseng* in rat tissues. *Biomed Chromatogr* 2006;20(4):327–35.
- [24] Antunes MB, Woodworth BA, Bhargava G, Xiong G, Aguilar JL, Ratner AJ, Kreindler JL, Rubenstein RC, Cohen NA. Murine nasal septa for respiratory epithelial air-liquid interface cultures. *Biotechniques* 2007;43(2):195–6. 8, 200 passim.
- [25] Cohen NA, Zhang S, Sharp DB, Tamashiro E, Chen B, Sorscher EJ, Woodworth BA. Cigarette smoke condensate inhibits transepithelial chloride transport and ciliary beat frequency. *Laryngoscope* 2009;119(11):2269–74.
- [26] Virgin F, Zhang S, Schuster D, Azbell C, Fortenberry J, Sorscher EJ, Woodworth BA. The bioflavonoid compound, sinupret, stimulates transepithelial chloride transport in vitro and in vivo. *Laryngoscope* 2010;120(5):1051–6.
- [27] Virgin FW, Azbell C, Schuster D, Sunde J, Zhang S, Sorscher EJ, Woodworth BA. Exposure to cigarette smoke condensate reduces calcium activated chloride channel transport in primary sinonasal epithelial cultures. *Laryngoscope* 2010;120(7):1465–9.
- [28] Woodworth BA, Antunes MB, Bhargava G, Palmer JN, Cohen NA. Murine tracheal and nasal septal epithelium for air-liquid interface cultures: a comparative study. *Am J Rhinol* 2007;21(5):533–7.
- [29] Cho DY, Skinner D, Zhang S, Fortenberry J, Sorscher EJ, Dean NR, Woodworth BA. Cystic fibrosis transmembrane conductance regulator activation by the solvent ethanol: implications for topical drug delivery. *Int Forum Allergy Rhinol* 2016;6(2):178–84.
- [30] Zhang S, Fortenberry JA, Cohen NA, Sorscher EJ, Woodworth BA. Comparison of vectorial ion transport in primary murine airway and human sinonasal air-liquid interface cultures, models for studies of cystic fibrosis, and other airway diseases. *Am J Rhinol Allergy* 2009;23(2):149–52.
- [31] In G, Ahn NG, Bae BS, Lee MW, Park HW, Jang KH, Cho BG, Han CK, Park CK, Kwak YS. In situ analysis of chemical components induced by steaming between fresh ginseng, steamed ginseng, and red ginseng. *J Ginseng Res* 2017;41(3):361–9.
- [32] Schroeder BC, Cheng T, Jan YN, Jan LY. Expression cloning of TMEM16A as a calcium-activated chloride channel subunit. *Cell* 2008;134(6):1019–29.
- [33] Liu L, Chu KK, Houser GH, Diephuis BJ, Li Y, Wilsterman EJ, Shastry S, Dierksen G, Birket SE, Mazur M, et al. Method for quantitative study of airway functional microanatomy using micro-optical coherence tomography. *PLoS One* 2013;8(1):e54473.
- [34] Birket SE, Chu KK, Houser GH, Liu L, Fernandez CM, Solomon GM, Lin V, Shastry S, Mazur M, Sloane PA, et al. Combination therapy with cystic fibrosis transmembrane conductance regulator modulators augment the airway functional microanatomy. *Am J Physiol Lung Cell Mol Physiol* 2016;310(10):L928–39.
- [35] Choi KT. Botanical characteristics, pharmacological effects and medicinal components of Korean *Panax ginseng* C A Meyer. *Acta Pharmacol Sin* 2008;29(9):1109–18.
- [36] Song Z, Kong KF, Wu H, Maricic N, Ramalingam B, Priestap H, Schnepel L, Quirke JM, Hoiby N, Mathee K. *Panax ginseng* has anti-infective activity against opportunistic pathogen *Pseudomonas aeruginosa* by inhibiting quorum sensing, a bacterial communication process critical for establishing infection. *Phytomedicine* 2010;17(13):1040–6.
- [37] Namkung W, Finkbeiner WE, Verkman AS. CFTR-adenylyl cyclase I association responsible for UTP activation of CFTR in well-differentiated primary human bronchial cell cultures. *Mol Biol Cell* 2010;21(15):2639–48.
- [38] Huang F, Zhang H, Wu M, Yang H, Kudo M, Peters CJ, Woodruff PG, Solberg OD, Donne ML, Huang X, et al. Calcium-activated chloride channel TMEM16A modulates mucin secretion and airway smooth muscle contraction. *Proc Natl Acad Sci U S A* 2012;109(40):16354–9.
- [39] Hwang SH, Shin TJ, Choi SH, Cho HJ, Lee BH, Pyo MK, Lee JH, Kang J, Kim HJ, Park CW, et al. Gintonin, newly identified compounds from ginseng, is novel lysophosphatidic acids-protein complexes and activates G protein-coupled lysophosphatidic acid receptors with high affinity. *Mol Cells* 2012;33(2):151–62.
- [40] Choi SH, Shin TJ, Lee BH, Hwang SH, Kang J, Kim HJ, Park CW, Nah SY. An edible gintonin preparation from ginseng. *J Ginseng Res* 2011;35(4):471–8.
- [41] Clarke LL, Grubb BR, Yankaskas JR, Cotton CU, McKenzie A, Boucher RC. Relationship of a non-cystic fibrosis transmembrane conductance regulator-mediated chloride conductance to organ-level disease in *Cftr(-/-)* mice. *Proc Natl Acad Sci U S A* 1994;91(2):479–83.
- [42] Rottgen TS, Nickerson AJ, Rajendran VM. Calcium-activated Cl<sup>-</sup> channel: insights on the molecular identity in epithelial tissues. *Int J Mol Sci* 2018;19(5).
- [43] Grayson J, Tipirneni KE, Skinner DF, Fort M, Cho DY, Zhang S, Prince AC, Lim DJ, Mackey C, Woodworth BA. Sinus hypoplasia in the cystic fibrosis rat resolves in the absence of chronic infection. *Int Forum Allergy Rhinol* 2017;7(9):904–9.
- [44] Tipirneni KE, Cho DY, Skinner DF, Zhang S, Mackey C, Lim DJ, Woodworth BA. Characterization of primary rat nasal epithelial cultures in CFTR knockout rats as a model for CF sinus disease. *Laryngoscope* 2017;127(11):E384–91.